J Appl Electrochem (2009) 39:713–717
DOI 10.1007/s10800-008-9714-0

ORIGINAL PAPER

Preparation and characterization of nanocrystalline Fe–Ni–Cr alloy electrodeposits on Fe substrate

Lijian Xu · Jingjing Du · Shuxun Ge · Nongyue He · Song Li

Received: 28 March 2008 / Accepted: 4 November 2008 / Published online: 22 November 2008

Abstract Fe–Ni–Cr alloy layers were prepared by electrodeposition from trivalent chromium plating bath in chloride-sulfate based solution. The influences of bath composition and plating parameters on the alloy electrodeposition process and the properties of deposited alloy were studied. The effects of plating parameters and bath composition such as current density, bath pH, bath temperature, the concentrations of $FeSO_4 \cdot 7H_2O$ and $CrCl_3 \cdot 6H_2O$ on the contents of Fe and Cr in Fe–Ni–Cr alloy layer were investigated. Electrodeposited Fe–Ni–Cr alloy layers on Fe substrate were characterized by X-ray diffraction (XRD), Electronic Differential System (EDS) and a CHI600B electrochemistry workstation. The composition of the Fe–Ni–Cr coatings depends on bath composition and plating conditions including pH, current density, and temperature. The internal structure of the alloy is nanocrystalline, the average grain size is 87 nm, and the corrosion resistance of the alloy layers is better than that of pure nickel layers.

Keywords Fe–Ni–Cr alloy · Corrosion resistance · Nickel · Electrodeposition

1 Introduction

Extensive demand from a wide spectrum of industrial applications has been the major driving force for research on corrosion resistant materials, leading to the development of chromium-based corrosion resistant alloys such as Cr–Ni, Cr–Fe and Cr–W–Ni [1–6]. However, few studies on electrodepositing Fe–Ni–Cr alloy on Fe substrate have been reported. Experiments show that it is difficult to increase the Cr content in the Fe–Ni–Cr alloy, because the deposition potential of Cr^{3+} is much more negative than that of Fe^{2+} and Ni^{2+}. Nickel, chromium, iron and their alloys are important engineering materials. They have unique properties, such as wear-resistance, corrosion resistance and electrocatalytic activity [7, 8]. In addition, the physicochemical properties of alloys are seriously affected by their composition and structure [9–12]. Therefore, reliable control of their composition and structure is an important issue. The operating conditions, such as current density, temperature, pH, use of organic additives, buffer capacity, concentration of all solution components, etc. lead to changes in the kinetics of electrodeposition, the composition and morphology of the coatings and their physicochemical characteristics.

The present study is aimed at obtaining Fe–Ni–Cr alloy layers on Fe substrates with good quality from a chloride-sulfate bath. Such a bath is not only cheap but also environmentally friendly. The effect of bath composition and some operating parameters on the composition of the Fe–Ni–Cr alloy layers are investigated. The properties and structure of the deposits are also examined.

L. Xu · S. Ge · N. He (✉) · S. Li
State Key Laboratory of Bioelectronics, School of Biological Science and Medical Engineering, Southeast University, Nanjing, People's Republic of China
e-mail: nyhe1958@163.com

L. Xu · J. Du · N. He · S. Li
Hunan Key Laboratory of Green Packaging and Application of Biological Nanotechnology, Hunan University of Technology, Zhuzhou, People's Republic of China

2 Experimental

2.1 Preparation of Fe–Ni–Cr alloy layers

A Fe foil was immersed in the solution containing 185 mL L^{-1} thick hydrochloric acid, 7.5 g L^{-1} OP emulsifier and 5 g L^{-1} 6-methenyl-4-ammonium to remove the greasy dirt and rust under 50 °C for 30 min. The Fe–Ni–Cr alloy layers were cathodically deposited on the Fe foil from a citrate plating bath. An optimized plating solution contained 40 g L^{-1} $FeSO_4 \cdot 7H_2O$, 220 g L^{-1} $NiSO_4 \cdot 6H_2O$, 45 g L^{-1} $NiCl_2 \cdot 6H_2O$, 25 g L^{-1} $CrCl_3 \cdot 6H_2O$, 45 g L^{-1} H_3BO_3, 30 g L^{-1} $C_6H_8O_7 \cdot H_2O$, 20 g L^{-1} $C_6H_5Na_3O_7 \cdot 2H_2O$. Two additives, i.e., lauryl sodium sulphate (0.06 g L^{-1}) and glucide (3 g L^{-1}), were used as wetting agent and brightener, respectively.

Electrodeposition was carried out at 10 to 18 A dm^{-2}, at a bath temperature from 298 to 318 K and pH from 1.5 to 3.5, the plating time was 15 min.

2.2 The composition and structure of the Fe–Ni–Cr alloy layers

The compositions of the Fe–Ni–Cr alloy layers were investigated by energy dispersive X-ray analysis (EDS). The microstructure and cross-sectional morphology of the Fe–Ni–Cr alloy layers were characterized by X-ray diffraction (XRD, Thermo X' TRAX-ray diffractometer with Cu $K\alpha_1$ irradiation) at a grazing angle of 4° with a step interval of 0.02°. Anodic curves of Fe–Ni–Cr alloy layers in 10% sulfuric acid solution (CHI600B electrochemistry workstation) were obtained to study the corrosion resistance of the alloy layers.

3 Results and discussion

3.1 Effect of the main processing parameters

3.1.1 Effect of the bath pH value

Figure 1 shows the effect of the bath pH value on contents of Fe and Cr in the Fe–Ni–Cr alloy layer. Increase in pH results in an increase in Fe and Cr contents in the Fe–Ni–Cr alloy layer to a maximum at 2.0, followed by a decrease. If the bath pH value is lower than 1.5, the electrochemical hydrogen evolution in the cathode becomes easy due to the high H^+ concentration in the bath, resulting in many blisters and pores in the surface of the alloy layer. However, when the bath pH value is higher than 2.0, the Fe and Cr contents in the Fe–Ni–Cr alloy layer decrease rapidly. This case is associated with the Cr^{3+} taking part in the hydroxyl polymerization [13, 14]. In a high pH value bath the reaction is easy and a condensation product of $Cr(OH)_3$ is obtained which is adsorbed on the cathode and, therefore, the reduction reactions of Cr^{3+} and Fe^{2+} are hindered, which causes the Cr and Fe contents in the alloy layers to decrease. Therefore, the bath pH value is suggested to be 2.0.

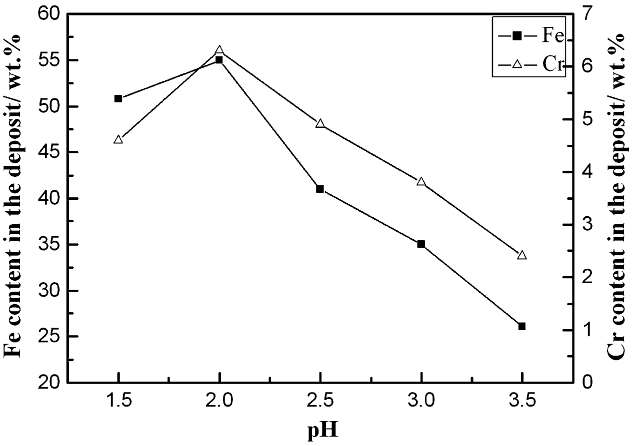

Fig. 1 Effect of the bath pH value on percentages of Cr and Fe in the deposits from bath containing 25 g L^{-1} $CrCl_3 \cdot 6H_2O$ and 40 g L^{-1} $FeSO_4 \cdot 7H_2O$ at current density 14 A dm^{-2}, $T = 303$ K and $t = 15$ min

3.1.2 Effect of bath temperature

The bath temperature should be set between 303 and 323 K to form a good adhesive and homogeneous Fe–Ni–Cr alloy layer. If the bath temperature is lower than 303 K, the alloy layer peels off easily. Figure 2 shows the effect of bath temperature on contents of Fe and Cr in the Fe–Ni–Cr alloy layer, and it is demonstrated that their contents decrease

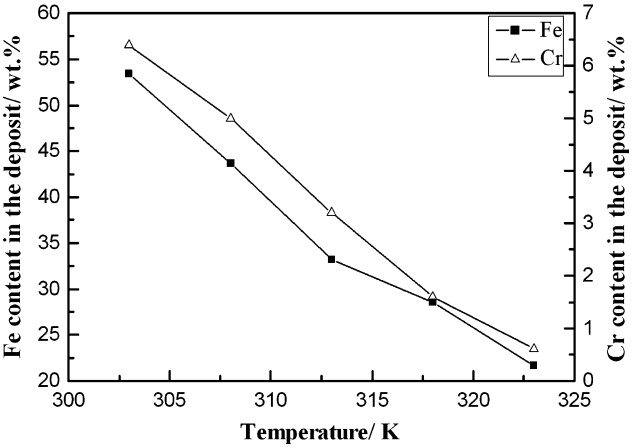

Fig. 2 Effect of the bath temperature on percentages of Cr and Fe in the deposits from bath containing 25 g L^{-1} $CrCl_3 \cdot 6H_2O$ and 40 g L^{-1} $FeSO_4 \cdot 7H_2O$ at current density A dm^{-2}, pH = 2.0 and $t = 15$ min

rapidly with increase in temperature. When the bath temperature is set over 323 K, the Cr content in the Fe–Ni–Cr alloy layer is less than 1 wt.%, and the Fe content is less than 20 wt.%. The influence of temperature on the composition of an alloy deposited in anomalous codeposition is determined by two opposing factors, i.e., polarization and diffusion. On increasing the temperature, the two factors tend to promote the electrodeposition of Ni^{2+}; the electrodeposition of Cr^{3+} and Fe^{2+} become relatively harder, resulting in an increase in Ni content in the deposit. Therefore, the bath temperature is suggested to be 303 K to obtain a high Cr content and good surface of Fe–Ni–Cr alloy layers.

3.1.3 *Effect of the current density*

The current density should be set between 10 and 18 A dm^{-2} to form a good adhesive and homogeneous Fe–Ni–Cr alloy layer. If the current density is set over 18 A dm^{-2}, a Fe–Ni–Cr alloy layer is formed, which is neither adhesive nor homogeneous and peels off easily. Figure 3 shows the effect of the current density on contents of Fe and Cr in the Fe–Ni–Cr alloy layer. It is shown that increasing the current density results in an increase in Fe and Cr contents in the Fe–Ni–Cr alloy layer, and contents of Fe and Cr reach a maximum at 14 A dm^{-2}, followed by a decrease. Therefore, the current density is suggested to be 14 A dm^{-2}.

3.1.4 *Effect of $CrCl_3 \cdot 6H_2O$ concentration*

Figure 4 shows that increase in the $CrCl_3 \cdot 6H_2O$ concentration in the bath increases the Cr content of the deposit up to a maximum, followed by a decrease, while the Fe content gradually decreases. At lower $CrCl_3 \cdot 6H_2O$ concentration, the Cr content in the alloy increases with increase in concentration of Cr^{3+}. When the $CrCl_3 \cdot 6H_2O$ concentration is increased further, to over 25 g L^{-1}, the Cr content decreases. This phenomenon should result from the high Cr^{3+} concentration in the bath promoting hydroxyl polymerization of Cr^{3+} and, therefore, Cr deposition is hindered. However, it is found that if the $CrCl_3 \cdot 6H_2O$ concentration is over 30 g L^{-1}, the alloy layer is neither adhesive nor homogeneous and peels off easily. Therefore, the $CrCl_3 \cdot 6H_2O$ concentration is suggested to be 25 g L^{-1} for obtaining a good Fe–Ni–Cr alloy layer with high Cr content.

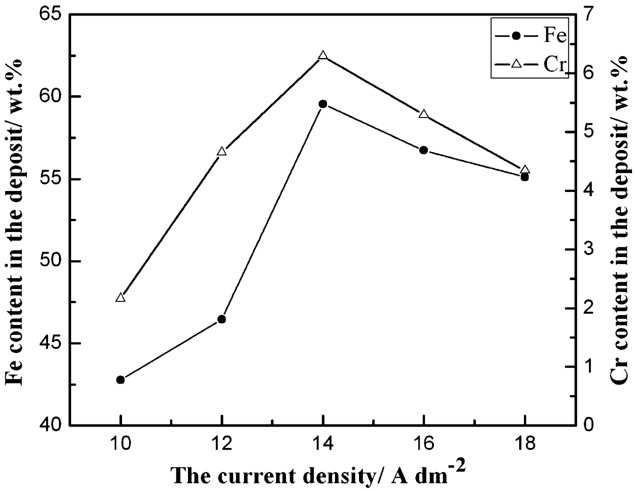

Fig. 3 Effect of the current density on percentages of Cr and Fe in the deposits from bath containing 25 g L^{-1} $CrCl_3 \cdot 6H_2O$ and 40 g L^{-1} $FeSO_4 \cdot 7H_2O$ at pH = 2.0, T = 303 K and t = 15 min

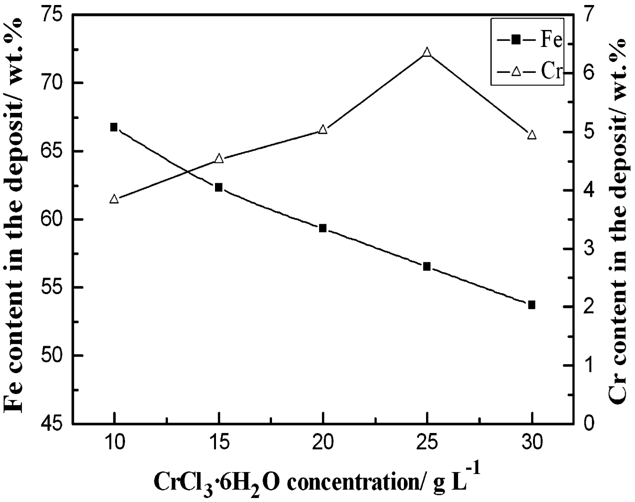

Fig. 4 Effect of the $CrCl_3 \cdot 6H_2O$ concentration on percentages of Cr and Fe in the deposits from bath containing 40 g L^{-1} $FeSO_4 \cdot 7H_2O$ at current density 14 A dm^{-2}, pH = 2.0, T = 303 K and t = 15 min

3.1.5 *Effect of $FeSO_4 \cdot 7H_2O$ concentration*

Figure 5 shows that increasing the $FeSO_4 \cdot 7H_2O$ concentration in the bath increases the Cr and Fe contents in the deposit. The Cr and Fe contents reach maxima at the $FeSO_4 \cdot 7H_2O$ concentration 40 g L^{-1}, then decrease. It seems that the electrodeposition of Cr^{3+} and Fe^{2+} on Fe substrate may promote each other, owing to an interactive synergy. The decrease in Cr and Fe contents in the alloy layer when the $FeSO_4 \cdot 7H_2O$ concentration is over 40 g L^{-1} can be attributed to the fact that Fe^{2+} species are easy to oxidize by Cr^{3+}. When the Fe^{2+} concentration in the bath is too high this results in a high Fe^{3+} concentration in the bath and hinders Cr and Fe deposition. Therefore, the $FeSO_4 \cdot 7H_2O$ concentration is suggested to be 40 g L^{-1}.

3.2 XRD examination of Fe–Ni–Cr alloy layers

Fe–Ni–Cr alloy electrodeposition under the above conditions yields a smooth, compact and bright layer. The XRD

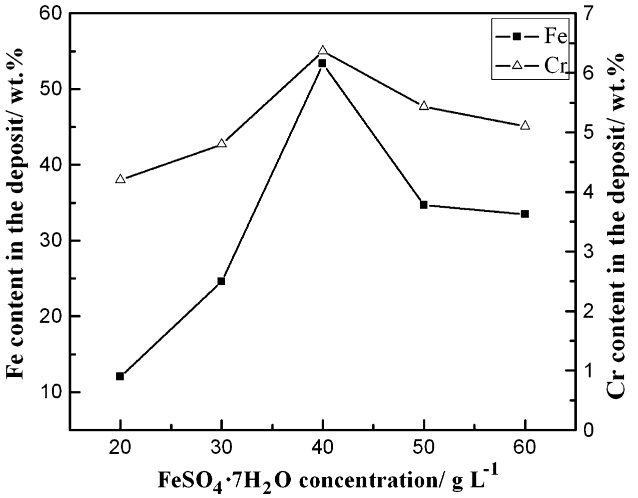

Fig. 5 Effect of the $FeSO_4 \cdot 7H_2O$ concentration on percentages of Cr and Fe in the deposits from bath containing 25 g L^{-1} $CrCl_3 \cdot 6H_2O$ at current density 14 A dm^{-2}, pH = 2.0, T = 303 K and t = 15 min

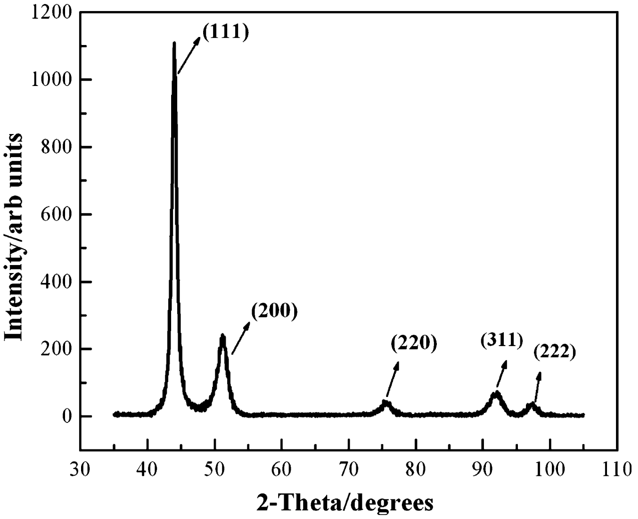

Fig. 6 X-ray diffraction patterns of electrodeposited $Fe_{54}Ni_{40}Cr_6$ alloy layer

pattern of a typical example of the $Fe_{54}Ni_{40}Cr_6$ alloy layer is shown in Fig. 6. The broadened peaks are observed at diffraction angles of around 43°, 51°, 76°, 93° and 97° corresponding to (111), (200), (220), (311) and (222) crystal planes of Fe–Ni–Cr phase, indicating that the microstructure of the alloy is crystalline. The average crystal size is estimated at 87 nm according to the Scherer formula [15, 16].

3.3 Corrosion resistance tests of Fe–Ni–Cr alloy layers

Figure 7 shows the anodic curves of Fe–Ni–Cr alloy layers in 10% sulfuric acid solution at 298 K. The passivation region is from 0.5 to 1.1 V, while the passivation region of the Ni layer is from 0.63 to 1.0 V. Thus the corrosion resistance of the alloy layers is better than that of pure nickel. The corrosion resistance of Fe–Ni–Cr alloy layers is improved because the Cr in the Fe–Ni–Cr alloy layers forms a refined Cr_2O_3 coating [17] on the surface by oxidation and the alloy layers possess a nanocrystalline structure and high adhesive strength to the Fe substrate.

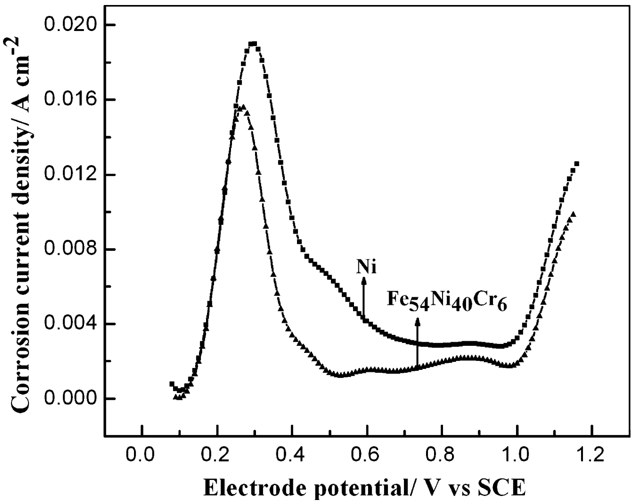

Fig. 7 The anodic curves of Fe-Ni-Cr alloy layer and Ni in the 10% sulfuric acid solution at 298 K. Sweep rate = 10 mV s^{-1}

4 Conclusions

We have described the preparation and characterization of nanocrystalline Fe–Ni–Cr alloy electrodeposits on Fe substrates. The optimal plating parameters and bath composition for Fe–Ni–Cr deposited coating good of quality are pH 2.0, current density 14 A dm^{-2}, temperature 303 K, $FeSO_4 \cdot 7H_2O$ 40 g L^{-1} and $CrCl_3 \cdot 6H_2O$ 25 g L^{-1}. XRD and anodic curves of Fe–Ni–Cr alloy layers in a 10% sulfuric acid solution show that the internal structure of the alloy is nanocrystalline, the average grain size is 87 nm and the corrosion resistance of the alloy layers is better than that of pure nickel. However, the Cr content in the Fe–Ni–Cr alloy layer is about 6 wt.%. In order to further improve the corrosion resistance of Fe–Ni–Cr alloy, we are studying the optimal additives to improve the Cr content.

Acknowledgments This research was financially supported by the National Natural Science Foundation of China (Nos. 60571032, 90606027), the Chinese 863 High Tech Project (No. 2007AA022007), the Hunan Science Foundation (2007FJ4050), Scientific Research Fund of Hunan Provincial Education Department (08C294), the Doctoral Program of Higher Education for Funding of China (No. 20050286014) and the Open Research Fund of State Key Laboratory of Bioelectronics, Southeast University.

References

1. Gu B, Tu JP, Zheng XH et al (2008) Surf Coat Technol 202:2189
2. Ishihara S, Notoya H, Okada A et al (2008) Surf Coat Technol 202:2085
3. Roldan A, Gómez E, Pané S et al (2007) J Appl Electrochem 37:575
4. Ferreira FBA, Silva FLG, Luna AS et al (2007) J Appl Electrochem 37:473
5. Wang HZ, Yao SW, Matsumura S (2002) Surf Coat Technol 157:166
6. Yuan YF, Tu JP, Wu HM et al (2007) J Appl Electrochem 37:249
7. Hu CC, Weng CY (2000) J Appl Electrochem 30:499
8. Hu CC, Bai A (2001) J Appl Electrochem 31:565
9. Kamel MM (2007) J Appl Electrochem 37:483
10. Osaka T (1999) Electrochim Acta 44:3855
11. Osaka T, Takai M, Ohashi K et al (1998) Nature 392:796
12. Yin KM (1997) J Electrochem Soc 144:1560
13. He XZ, Gong ZQ, Jiang HY (2000) Trans Nonferrous Met Soc 10:95
14. Xu LJ, Gong ZQ, Tang JX et al (2007) J Cent South Univ Technol 14(2):181
15. Pakokthom C, Rujijanagul G, Tunkasiri T (1999) J Mater Sci Lett 18:747
16. Liu YP, Zhu YJ, Zhang YH et al (1997) J Mater Chem 7(5):787
17. Cunha L, Andritschky M, Pischow K et al (2002) Surf Coat Technol 153:160